

VIBRATIONAL ANALYSIS AND OPTIMIZATION OF BIPOLAR PLATES IN PEMFCs: A SIMULATION AND OPTIMIZATION BASED STUDY

Longqian (Derek) Zhang¹, Yuxuan Liu¹, Utkarsh Chadha², Kamran Behdinan^{2*}

¹Department of Mechanical and Industrial Engineering, Faculty of Applied Sciences and Engineering, University of Toronto, Toronto, Canada, M5S 3G8

²Advanced Research Laboratory for Multifunctional Lightweight Structures (ARL-MLS), Department of Mechanical and Industrial Engineering, University of Toronto, Toronto, ON, M5S 3G8, Canada

*e-mail address: behdinan@mie.utoronto.ca;

Abstract—PEMFCs have been replacing heavy batteries, to reduce the weight penalty, which would also result in lower energy consumption. It is vital to study the effects of their environment, as these fuel cells would experience extensive vibrations be it inside a car, ship or any other machine which is powered by it. This study covers the essentials about the PEMFCs and discovers dimensions to evaluate the vibrational behavior of bipolar plates using finite element modeling (FEM) and multi-objective optimization methods like design of experiments (DoE), and particle swarm optimization (PSO). Furthermore, this study focuses solely on vibration-related analysis through thorough analysis.

Keywords- *Vibrational Analysis; PEMFCs; Bipolar Plates, DoE, Particle Swarm Optimization; Simulations.*

I. INTRODUCTION

Bipolar plates, in a PEMFC, play a crucial role in uniform distribution of reactant gases and conducting electric currents across cells, while also maintaining the structural and mechanical integrity of the entire fuel cell [2]. Typically, the chosen material ranges from graphite, metallic alloys or carbon composites, as the bipolar plates are supposed to withstand chemical stresses, thermal stresses and mechanical vibrations during the operations [3, 4]. PEMFCs are widely recognized for their high efficiency and low emissions, making them suitable for automotive, maritime, and stationary power systems [5].

Bipolar plates play a crucial role in uniform distribution of reactant gases and conducting electric currents across cells, while also maintaining the structural and mechanical integrity of the entire fuel cell [2]. These plates conduct the electrons generated at the anode to the external circuit, allowing for the flow of electricity. Bipolar plates

contain flow channels that distribute hydrogen and oxygen/air uniformly across the anode and cathode, respectively [6]. These channels are crucial for maximizing the reaction surface area and ensuring efficient reactant utilization. Alongside these, it helps in managing the water produced at the cathode, ensuring that the water does not flood the cell and disrupts the flow of gases [7]. They also help maintain membrane hydration, which is vital for efficient proton conduction. Bipolar plates contribute to heat dissipation, preventing overheating of the cell and ensuring stable operation [8]. Some designs include cooling channels within the plates to control the temperature of the fuel cell stack. They provide structural integrity and ensure proper compression of the MEA, maintaining contact for better electrical conduction [9].

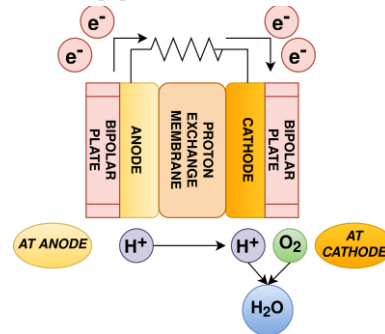


Figure 1. An Overview of the functioning of a PEMFC, and the role of bipolar plates.

Figure 1 shows the functioning of a generic PEMFC, with the role of bipolar plates explained in exhaustive manner. The vibration-induced effects on bipolar plates should be investigated for the material fatigue assessment, misalignment of components, and gas leaks that can adversely affect the

performance of the fuel cell [10]. There is a high possibility that water management and electrochemical reactions are hindered leading to efficiency issues.

Typically, the chosen material ranges from graphite, metallic alloys or carbon composites, as the bipolar plates are not only supposed to withstand chemical and thermal stresses, but also mechanical vibrations during the operations [3, 11]. Graphite offers excellent corrosion resistance but suffers from low mechanical strength, making it susceptible to cracking under prolonged vibrations [8]. Metallic bipolar plates, such as stainless steel and titanium, exhibit superior mechanical resilience but require coatings to enhance corrosion resistance and prevent hydrogen permeability [11].

Vibrational stress can lead to delamination of bipolar plates, affecting gas diffusion and electrical conductivity, ultimately degrading PEMFC efficiency. Fatigue-induced material failure in PEMFCs is a key challenge, as cyclic vibrations accelerate crack propagation in brittle materials such as graphite [9]. Ensuring a sufficiently high natural frequency in PEMFCs is crucial to preventing resonance, which can significantly amplify mechanical stresses and shorten the system's lifespan. Mechanical degradation of PEMFC components due to vibrations is a major factor limiting their adoption in high-mobility applications, necessitating advanced structural optimization techniques [10].

This study aims to convert Proton Exchange Membrane Fuel Cells (PEMFCs) for varied applications, addressing the challenges posed by constant vibrations on these fuel cells [12]. Optimization approaches, such as genetic algorithms and ant colony optimization, are utilized to improve performance by balancing natural frequency and mass [9, 10].

II. CONCEPTUAL DESIGN & PRELIMINARY REQUIREMENTS

PEMFCs produce clean, efficient energy, however the variable environment can affect their efficiency. Understanding ship-induced vibrations (lateral, longitudinal, and vertical) is crucial for ship reliability. The goal is to improve maritime PEMFC system design and durability.

Figure 2 shows a geometric single-channel PEMFC model. In Table I, the bipolar plate, gas diffusion layers (GDL), catalytic layers, and proton exchange membrane (PEM) are crucial [12].

These components are necessary for electrochemical reactions that generate electricity, water, and heat from hydrogen and oxygen. The PEMFC generates electricity by transferring protons through the membrane and electrons through an external circuit. Figure 3 shows the displacement patterns of harmonic vibrations—lateral, longitudinal, and

vertical—applied using dynamic mesh technology and user-defined functions (UDF). The vibrations simulate ship conditions for the PEMFC.

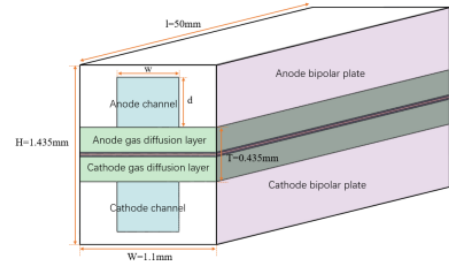


Figure 2. A Single-channel PEMFC model. Adapted with Permission from [12].

TABLE I. Model dimension. Adapted with Permission from [12].

Geometric parameter	Numerical value (mm)
Bipolar plate	Maximum thickness:0.5
	Minimum thickness: 0.1
Channel	Width (w): 0.5
	Depth (d):0.4
Gas Diffusion Layer (T_{gai})	Thickness: 0.2
Catalytic layer (T_{cl})	Thickness: 0.01
Proton exchange membrane (T_{pem})	Thickness: 0.015

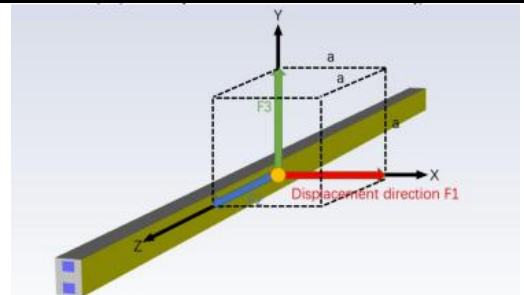


Figure 3. Vibration load displacement pattern. Adapted with Permission from [22].

III. ANALYSIS APPROACH

The study by Guo et al. [12], employs a comprehensive approach to assess the dynamic behavior of Proton Exchange Membrane Fuel Cells (PEMFCs) subjected to vibrational loads, specifically in the context of various applications. To achieve a thorough analysis, we will utilize three distinct methodologies: continuous system analysis, and finite element modeling (FEM).

Continuous system analysis using SolidWorks to model PEMFC components as continuous elastic media is the first stage. PDEs are used to characterize the spatial distribution of stress, strain, and deformation across the system under vibrational excitation. Continuous system analysis is appropriate for studying the global dynamic response of thin-walled systems like the PEM, where material continuity and boundary conditions are crucial to structural performance.

Next, use ANSYS FEM to analyze the PEMFC's vibrational properties at high resolution. FEM discretizes the PEMFC's complicated geometries and heterogeneous materials into finite elements for precise vibrational response computation. This method is necessary to detect natural frequencies, mode shapes, and forced vibrational behavior of the system, allowing thorough analysis of localized impacts like stress concentrations and fuel cell failure spots under operational settings.

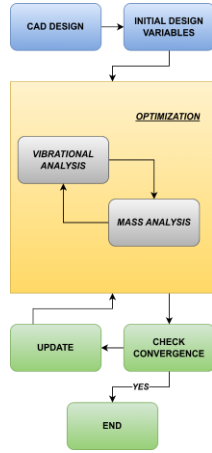


Figure 4. Flow chart for design progress.

Finally, multi-objective optimization can be used to enhance the design of PEMFCs. It can enable the simultaneous attainment of optimal outcomes for both mass (m) and natural frequency (ω_n). The goals can be set to optimize the natural frequency (ω_n) while reducing the mass (m). The design variables consist of the dimensions of various layers within the PEMFC. A higher natural frequency guarantees that the fuel cell components are less susceptible to entering a resonance state.

Considering the multiple degrees of freedom in this model, it is possible that the FEA results will have multimodal characteristics. At this time gradient-based algorithms are unsuitable because gradient-based algorithms may define a local optimum as a global optimum. Alternatively, we could implement genetic algorithms or ant colony algorithms (Figure 4).

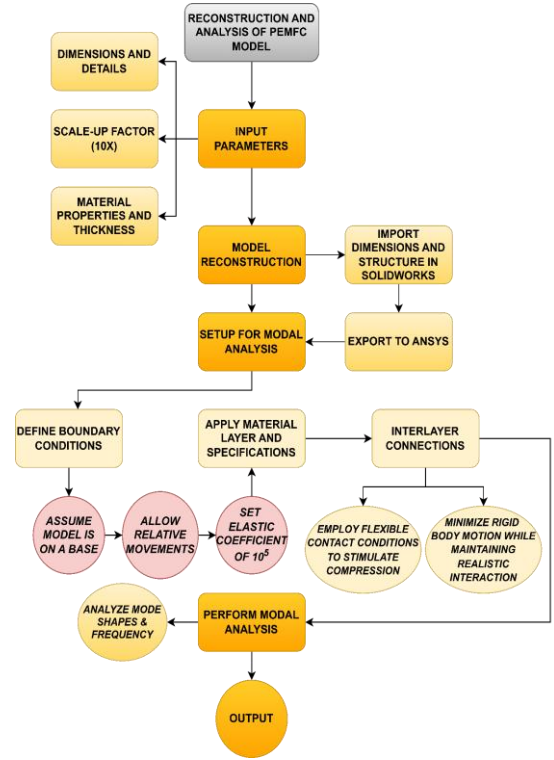


Figure 5. Finite Element Method: Essential Mapping for Implementation.

IV. METHODOLOGY: DETAILS & ASSUMPTIONS

A. Experimental Details for FEM Analysis

Figure 5 shows the Single-channel PEMFC model from Guo et al. [12] recreated in SolidWorks and increased by a factor of 10 to fix its small size. Further modal analysis was done in ANSYS. In order to simulate actual boundary conditions, the model was assumed to be on a base and allowed relative movement with an elastic coefficient of 105. Table II lists layer material and thickness. Flexible contact conditions were used for interlayer connections to simulate PEMFC mechanical compression. This strategy reduced rigid body motion while maintaining layer interaction.

TABLE II. Materials, and their Details Used in Simulation Assumptions for Specific PEMFC Model Components.

Components	Material	Initial Thickness (mm)	Mass (g)
Bipolar Plate	Graphite	5	3.92
Channel	Porous Carbon	4	0.44
Gas Diffusion Layer	Platinum	2	23.595
Proton Exchange Membrane	Nafion	0.15	0.12524

B. Experimental Details for FEM Analysis

This approach disregards the effects of damping. This assumption aligns with both the finite element method (FEM) system approach, wherein damping is typically neglected to facilitate modal analysis and concentrate on the undamped natural frequencies.

The PEMFC model is supposed to be situated on a ground surface, regarded as a fixed support. Nevertheless, the interaction between the model and the ground is not seen as completely bound. An elastic contact condition is utilized to more accurately depict real-world situations where the model exhibits some flexibility or restricted sliding at the interface.

In the PEMFC model, the layers are presumed to be in elastic contact with one another. This assumption indicates differences in production methods, such as pressing or hot assembly, leading to layers being mechanically squeezed instead of firmly connected. The elastic contact condition considers the possible flexibility and localized interaction among layers.

V. OPTIMIZATION

A. Particle Swarm Optimization

PSO began with computer simulations of bird flocking and fish schooling. Based on these behaviors, the system simulates particle movement and social interaction in a search zone. Swarm particle initialization involves setting their starting positions and velocities. Initial locations and velocities are randomly assigned to each particle, representing a solution [13].

Velocity update formula is [13]:

$$v_i^{t+1} = wv_i^t + c_1r_1(p_i^t - x_i^t) + c_2r_2(g^t - x_i^t) \quad (1)$$

where:

v_i^{t+1} : velocity of particle i at time t+1

w: inertia weight

c_1c_2 : acceleration coefficients

r_1r_2 : random number between 0~1

p_i^t : personal best position

g_i^t : global best position

x_i^t : position of particle i at time t

The position of each particle is updated using [13]:

$$x_i^{t+1} = x_i^t + v_i^{t+1} \quad (2)$$

The PSO algorithm randomly initializes particle positions and velocities, assesses each particle's fitness value based on its current position, and updates personal and global beats by comparing the current fitness value to the historical best values [13]. Particle velocities and positions are then modified using velocity and position update equations. This algorithm repeats until a termination requirement is fulfilled, such as a maximum iteration count or a fitness threshold [13].

B. Multi objective optimization

MOO optimizes many objective functions at once. MOO is an efficient way to manage trade-offs between

conflicting goals. Many Pareto-optimal strategies are available [14]. With its many benefits, multi-objective optimization is essential. It provides holistic solutions that consider multiple goals, providing deeper insights. By focusing on model complexity, MOO often creates simpler, easier-to-understand models. This helps people make educated decisions by offering a number of options, including trade-offs, so they can weigh numerous variables. MOO also allows dynamic system modeling with varying preferences and limits. It can also increase predicted performance by optimizing models on several factors rather than accuracy [14].

VI. RESULTS AND DISCUSSIONS

A. Outcomes of FEM Analysis

Figure 6 illustrates the meshing results, including an element size of 0.8mm, including a total of 127,422 elements and 204,318 nodes, and Table III presents the initial natural frequency obtained. Furthermore, forced vibration analysis was conducted over the natural frequency spectrum from modes 1 to 10 (0~2000Hz) under 1000N force, resulting in the maximum amplitude, which is also included in Table III.

TABLE III. Materials, and their Details Used in Simulation Assumptions for Specific PEMFC Model Components.

Methods	1st Natural Frequency (Hz)	Max Displacement (m)	Force vibration Max displacement (m)
Continuum (FEM)	76.6	1.4178e-004	9.5606e-006

Figure 7 illustrates the displacement amplitude of the anode bipolar plate subjected to harmonic excitation over a frequency range of 0 to 2000 Hz. The x-axis denotes frequency (Hz), while the y-axis indicates displacement amplitude (m). The peak displacement occurs at roughly 1800 Hz with an amplitude of 9.56×10^{-6} m, signifying a resonance point. Comprehending this behavior is essential to prevent resonance during the design phase and enhance the structural integrity of the PEMFC system.

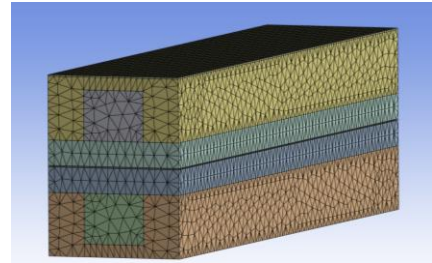


Figure 6. Mesh results from ANSYS.

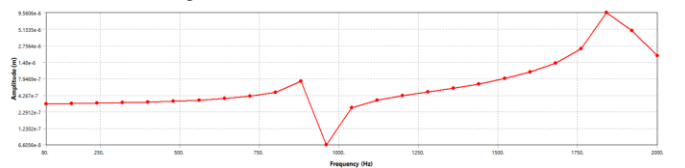


Figure 7. Amplitude VS Frequency under 1000N.

B. Outcomes of Optimization: Design of Experiments (DoE)

By completing the finite element study, the next step involved multi objective design optimization to maximize the first natural frequency ($f_w(x)$) while concurrently decreasing the mass ($f_m(x)$) of the PEMFC. The design variables consisted of the thicknesses of several layers, with constraints imposed on these thicknesses as specified below:

$$\begin{aligned} \text{Minimize:} & \quad f_m(x), -f_w(x) \\ \text{By varying:} & \quad x = [T_c, T_{bp}, T_{pem}, T_{gdl}] \\ \text{Subject to:} & \quad 3.6 < T_c < 4.4 \\ & \quad 4.5 < T_{bp} < 5.5 \\ & \quad 0.1035 < T_{pem} < 0.1265 \\ & \quad 1.8 < T_{gdl} < 2.2 \end{aligned}$$

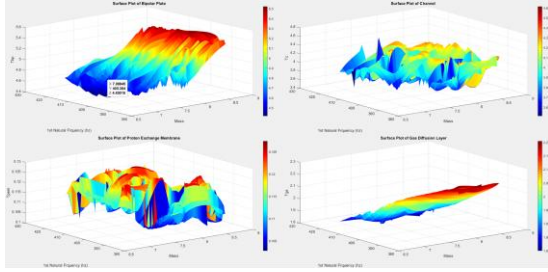


Figure 8. 3D surface plots of Layer thickness vs Mass and 1st Natural frequency.

In iSIGHT, the Design of Experiments (DOE) method was used to evaluate 100 design points against design constraints. Different layer thicknesses affect mass and natural frequency, as demonstrated in three-dimensional charts in Figure 8. The findings show a multimodal relationship where gradient-based algorithms may fail due to local minima convergence.

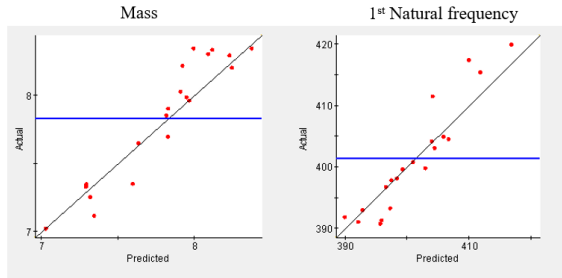


Figure 9. Validation of the Kriging-Based Surrogate Model: Predicted vs. Actual Outcomes

Kriging was used to create a proxy model for the design space. This strategy reduced computing costs by replacing direct finite element assessments with the surrogate model. The surrogate model's accuracy is shown in Figure 9 by comparing predicted values to simulated results. Particle Swarm Optimization (PSO), which excels at multimodal design domains, was used for multi-objective optimization. The flowchart describes the optimization process. This solution balanced computer efficiency with design goals.

Running 10,000 iterations with a surrogate model to lower processing costs, Particle Swarm Optimization (PSO) efficiently handled multimodal difficulties in this work. Forty

main points were chosen to exhibit convergence, as Figure 10 shows, the stabilization of important variables toward the best solution.

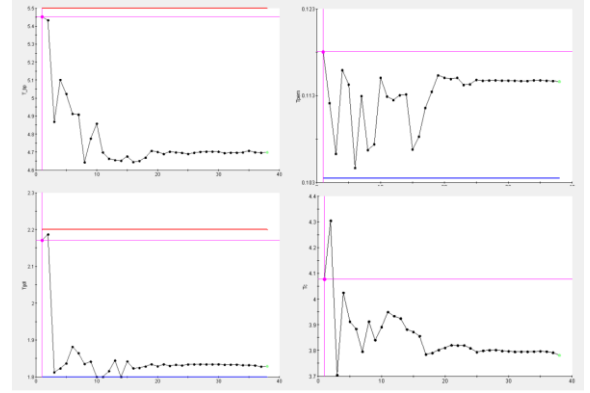


Figure 10. Convergence for PSO iteration.

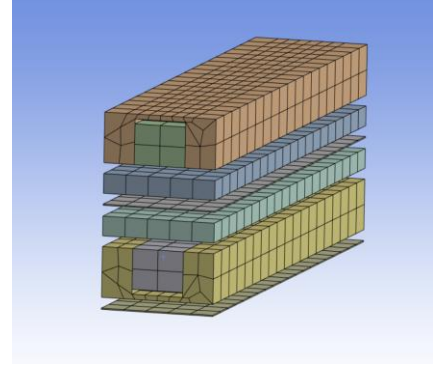


Figure 11. Optimized CAD model of the PEMFC.

TABLE IV. Optimization Results of Layer Thickness, First Natural Frequency, and Total Mass Using PSO.

Layer	Thickness (mm)		1st w_n (Hz)		Mass (g)	
	Initial	Optimized	Initial	Optimized	Initial	Optimized
Bipolar plate	5	4.6987	76.6	420.52	3.920	3.419
Channel	4	3.7818			0.440	0.416
Gas Diffusion layer	2	1.8289			23.595	23.576
Proton Exchange Membrane	0.15	1.3463			0.125	0.1248
Total Mass					56.035	50.947

The values in Table IV reveal significant changes: the first natural frequency rose from 76.6 Hz to 420.52 Hz, and the mass dropped generally by 9%, from 56.0352 g to 50.94686 g. Within design constraints, these gains came from varying the thicknesses of the bipolar plate, channel, gas diffusion layer, and proton exchange membrane. The resulting CAD model is shown in Figure 11.

The findings validate that the integration of Particle Swarm Optimization with surrogate modeling is exceptionally efficient for multi-objective optimization in modal analysis. The improved design markedly improves the structural and functional performance of the PEMFC by balancing the trade-off between enhancing natural frequency and decreasing mass.

VII. CONCLUSIONS

The optimization of the PEMFC design, integrating Particle Swarm Optimization (PSO) with surrogate modeling, achieved a substantial enhancement in performance by increasing the first natural frequency from 76.6 Hz to 420.52 Hz while reducing mass by 9%. This was accomplished through precise adjustments to layer thickness within specified constraints, validated by Kriging-based surrogate modeling and efficient computational workflows. The results demonstrate a significant balance between structural integrity and lightweight design, highlighting the efficacy of PSO in addressing multimodal optimization challenges for advanced engineering systems.

VIII. FUTURE DIRECTIONS

There is a need to study damping effects into the vibration analysis to enhance the realism of the simulations and better predict operational behaviors. Further exploration of alternative materials and composite structures for PEMFC components could optimize performance while reducing weight. Expanding the surrogate modeling framework to include additional manufacturing constraints and environmental factors (e.g., thermal and moisture effects) would improve the design's validity and strengthen the reliability of the results obtained. Additionally, implementing real-world experimental validation of the optimized model can ensure its applicability in practical scenarios.

REFERENCES

- [1] Tawfik, H., Hung, Y., & Mahajan, D. (2007). Metal bipolar plates for PEM fuel cell—A review. *Journal of power sources*, 163(2), 755-767.
- [2] Dhakate, S. R., Sharma, S., Borah, M., Mathur, R. B., & Dhami, T. L. (2008). Expanded graphite-based electrically conductive composites as bipolar plate for PEM fuel cell. *International journal of hydrogen energy*, 33(23), 7146-7152.
- [3] Hou, Y., Hao, D., Shen, J., Li, P., Zhang, T., & Wang, H. (2016). Effect of strengthened road vibration on performance degradation of PEM fuel cell stack. *International Journal of Hydrogen Energy*, 41(9), 5123-5134.
- [4] Joseph, S., McClure, J. C., Chianelli, R., Pich, P., & Sebastian, P. J. (2005). Conducting polymer-coated stainless steel bipolar plates for proton exchange membrane fuel cells (PEMFC). *International Journal of Hydrogen Energy*, 30(12), 1339-1344.
- [5] Bozorgnezhad, A., Shams, M., Kanani, H., Hasheminasab, M., & Ahmadi, G. (2016). Two-phase flow and droplet behavior in microchannels of PEM fuel cell. *International Journal of Hydrogen Energy*, 41(42), 19164-19181.
- [6] Musse, D., & Lee, D. (2024). Computational evaluation of PEMFC performance based on bipolar plate material types. *Energy Reports*, 11, 4886-4903.
- [7] Liu, W., Qiu, D., Peng, L., Yi, P., & Lai, X. (2020). Mechanical degradation of proton exchange membrane during assembly and running processes in proton exchange membrane fuel cells with metallic bipolar plates. *International Journal of Energy Research*, 44(11), 8622-8634.
- [8] Yan, X., Hou, M., Zhang, H., Jing, F., Ming, P., & Yi, B. (2006). Performance of PEMFC stack using expanded graphite bipolar plates. *Journal of power sources*, 160(1), 252-257.
- [9] Wilberforce, T., Olabi, A. G., Monopoli, D., Dassisti, M., Sayed, E. T., & Abdelkareem, M. A. (2023). Design optimization of proton exchange membrane fuel cell bipolar plate. *Energy Conversion and Management*, 277, 116586.
- [10] Liu, B., Liu, L. F., Wei, M. Y., & Wu, C. W. (2016). Vibration mode analysis of the proton exchange membrane fuel cell stack. *Journal of Power Sources*, 331, 299-307.
- [11] Asri, N. F., Husaini, T., Sulong, A. B., Majlan, E. H., & Daud, W. R. W. (2017). Coating of stainless steel and titanium bipolar plates for anticorrosion in PEMFC: A review. *International Journal of Hydrogen Energy*, 42(14), 9135-9148.
- [12] Guo, S., Zhao, Y., Wang, X., Lin, F., & Xu, Z. (2024). Leakage mechanism model of proton exchange membrane fuel cell sealing structures under vibration conditions. *International Journal of Green Energy*, 1-11.
- [13] Tang, J., Liu, G., & Pan, Q. (2021). A review on representative swarm intelligence algorithms for solving optimization problems: Applications and trends. *IEEE/CAA Journal of Automatica Sinica*, 8(10), 1627-1643.
- [14] Zakaria, M. Z., Jamaluddin, H., Ahmad, R., & Loghmanian, S. M. (2012). Comparison between multi-objective and single-objective optimization for the modeling of dynamic systems. *Proceedings of the institution of mechanical engineers, part i: journal of systems and control engineering*, 226(7), 994-1005.